Available online at www.sciencedirect.com
SCIENCE DIRECT®
Physica A 326 (2003) 322–332
PHYSICA A
www.elsevier.com/locate/physa

Hedgehog–antihedgehog pair annihilation to a static soliton

P.E. Cladis[a,*], Helmut R. Brand[a,b]

[a] *Advanced Liquid Crystal Technologies Inc., P.O. Box 1314, Summit, NJ 07902, USA*
[b] *Theoretische Physik III, Universität Bayreuth, D-95440 Bayreuth, Germany*

Received 30 January 2003

Abstract

We experimentally demonstrate that, for sufficiently small perturbations, a hedgehog (H) and antihedgehog ($\bar{H}$) point defect in nematic liquid crystals can be asymptotically free. For larger external perturbations, we find that the annihilation dynamics of an $H\bar{H}$ pair to a static soliton is asymmetric and shows two time regimes. A model for the experimental observations in the absence of smectic A fluctuations is proposed.

PACS: 61.30.Jf; 05.70.Ln; 02.40.−k

Keywords: Solitons in liquid crystals; Point defect dynamics; Non-equilibrium phenomena

1. Introduction

The study of the dynamics of defects and their interactions e.g. Refs. [1–4] in 3D anisotropic liquids is important because it enables well-controlled experiments in simple geometries to substantiate the physical consequences of topological constraints and underlying symmetries. Especially in the 3D anisotropic liquids, liquid crystals [5] and superfluid ^{3}He [6], the annihilation dynamics of defects has helped develop understanding of the basic laws obtained from nonlinear field theories (see e.g. Ref. [7]).

Here, we show experimentally, for the first time, that the annihilation dynamics of originally asymptotically free point defect pairs (Fig. 1), called hedgehogs (H) and antihedgehogs ($\bar{H}$), is asymmetric when driven by a sufficiently large perturbation.

* Corresponding author.
E-mail address: cladis@alct.com (P.E. Cladis).

0378-4371/03/$ - see front matter © 2003 Published by Elsevier B.V.
doi:10.1016/S0378-4371(03)00254-1

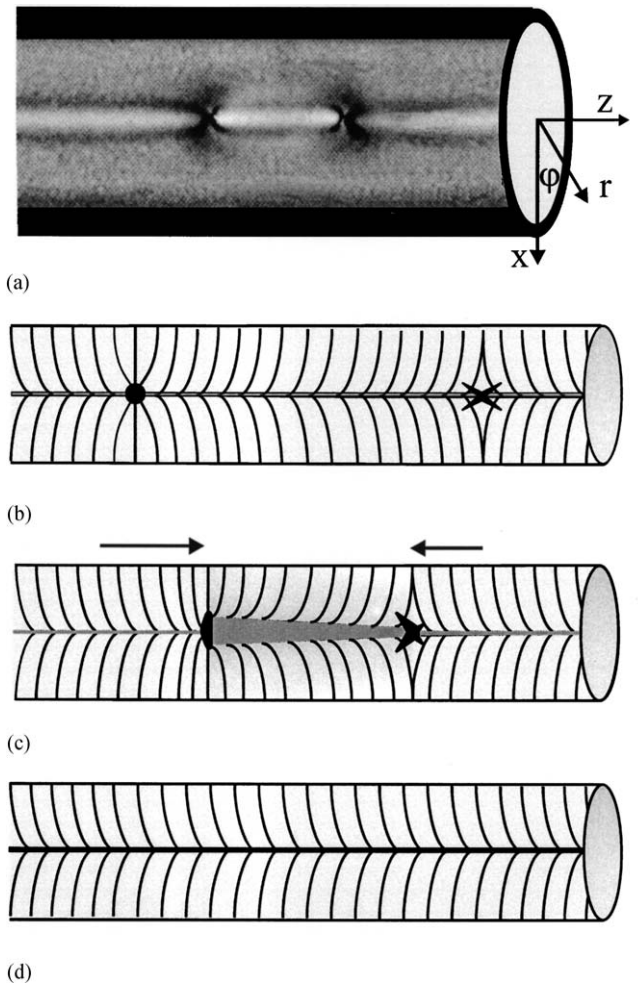

Fig. 1. (a) Cylindrical reference frame and snapshot viewed with polarizers crossed 45° to $\hat{\mathbf{z}}$ of a hedgehog (H) and antihedgehog ($\bar{H}$) in the process of annihilating in a capillary of diameter, $d = 149$ μm. Note the difference in contrast between H and $\bar{H}$ in the center of the capillary compared to that outside of the $H\bar{H}$ pair. (b) Sketch of the director configuration where $\hat{\mathbf{n}}$ is radial at the capillary walls and axial at $r = 0$ for an asymptotically free hedgehog (left) and antihedgehog (right) in a diameter plane rotationally symmetric about $\hat{\mathbf{z}}$. $\hat{\mathbf{n}}$ is parallel to the lines. (c) A perturbation induces a more energetic region between the $H\bar{H}$ pair (shown shaded) setting them on an annihilation course to remove it. (d) Sketch of the static soliton left behind after $H\bar{H}$ pair annihilation.

This turns out to be consistent with a model making use of the general solutions for nematics in the cylindrical geometry with well-defined boundary conditions [8]. [1]

[1] While Cladis and Kléman discuss all cases, the infinite number of symmetry breaking solutions of interest here are those they designated $A^2 = 1/\sin^2\alpha \geqslant 1$ as these solutions have a possible core structure that does not require introducing other singularities.

Point defects are topologically (and therefore physically) different from line defects. This is true even if the elastic field around a line defect varies only in a plane perpendicular to the line, the so-called planar line defects. While the energy per unit length of planar line defects logarithmically diverges both as one approaches and goes away from the line, the energy per unit length of a point defect is constant[2]. As a result, there is no interaction energy to drive point defects to annihilate as there is in the case of line defects. At equilibrium, point defects are asymptotically free.

This raises the question: how come point defects annihilate? In fact, point defects annihilate very easily [9]. We will argue that, as the creation of point defects requires pushing the system out of equilibrium, they have a chance to rapidly annihilate before the system reaches equilibrium. In the best-controlled geometry for observing point defects [10], stationary point defect pairs are infrequent objects at long times: asymptotic freedom is a state that must be delicately cultivated.

For example, as the time constant for elastic relaxation to equilibrium scales with the square of a characteristic sample dimension and the magnitude of the nematic orientational diffusion constant (given by the ratio of a viscous coefficient to an elastic constant) "thinner" samples relax faster to equilibrium than "thicker" ones. Thus from an experimental perspective, sample dimension and the visco-elastic properties of the nematic liquid crystal must be carefully selected to observe point defects and their annihilation dynamics over long times (1 day). The observation of asymptotic freedom depends in addition on finely tuned experimental control, e.g., sample preparation, polarized light optics, temperature control and a computer controlled imaging system that enables fast data sampling over long times.

While the fact that unperturbed $H\bar{H}$ pairs experience no interaction force when sufficiently far apart has been understood for a long time now [9,11], it has only very recently been numerically verified [12]. We also note that asymptotically free $H\bar{H}$ pairs are physically distinguishable from monopole–antimonopole ($m\bar{m}$) pairs bound to each other by a disclination loop whose relaxation controls $m\bar{m}$ pair annihilation [13]. We also note the recent growing interest in the interaction of planar line defects of strength 1/2 in nematics [14–16], a situation different from point defect dynamics.

[2] In a sphere of radius R, the defect elastic energy for the hedgehog is $E_H = 8\pi K_1 R + E_c^H$, where E_c^H is a core energy. For the antihedgehog, we have $E_{\bar{H}} = 8\pi R(K_1 + 2(K_3 + K_{24})/3)/5 + E_c^{\bar{H}}$ where the K_{24} surface term, is evaluated on $r = R$. As the total energy, E, stored in the nematic director field around an H or $\bar{H}$ scales with R, there is no net attractive force driving them to annihilate. For comparison, the energy/unit length of a static soliton in the cylindrical geometry: $E_{\mathscr{S}\mathscr{S}} = \pi(2K_1 + K_3 k/\tan k)$ with $\tan^2 k = (K_3 - K_1)/K_1$ [8]. The one constant approximation (all elastic constants the same) enables a rough comparison of the relative energies of the point defects and the static soliton. Obviously, better estimates require 2D calculations of H and $\bar{H}$ energies in the cylindrical geometry which is outside the scope of this paper. Ignoring constant terms and core energies (i.e., E_c), the energy/length of a static soliton in units of πK is $E_{\mathscr{S}\mathscr{S}}/\pi K = 2$ [8]. That of the hedgehog is $E_H/\pi KR = 8$ and that of the antihedgehog is $E_{\bar{H}}/\pi KR = 8/3$. While the hedgehog energy per length is larger than that of the static soliton, that of the antihedgehog is closer to that of the static soliton and 1/3 that of the hedgehog.

2. Point defects in nematic liquid crystals

For many organic materials, an isotropic liquid transforms to a nematic liquid crystal phase at a nematic–isotropic transition temperature, T_{NI}. The nematic phase is characterized by long-range orientational order in a preferred direction, $\hat{\mathbf{n}}$. $\hat{\mathbf{n}}$ is a unit vector, called the director, for which $\hat{\mathbf{n}}$ and $-\hat{\mathbf{n}}$ are indistinguishable. Because of the constraint, $\hat{\mathbf{n}}^2 = \mathbf{1}$, deviations in $\hat{\mathbf{n}}$ from a uniform state are nonlinear. A smectic A phase, whose order parameter is a 1D density wave $\|\hat{\mathbf{n}}$, at a lower temperature, T_{NA}, gives a strong temperature dependence to certain of the nematic's material constants [4] (see e.g. Ref. [17]). For example, the nematic elastic constant for bend, K_3 (as well as its rotational viscosity, γ_1), diverges as $T \to T_{NA}$ while that for splay, K_1, is unaffected.

Point defects were first observed [10] in cylindrical capillaries of radius R prepared so that $\hat{\mathbf{n}}$ is radial at $r = R$ (Fig. 1). With these boundary conditions, the director field equation has an infinite number of spontaneous symmetry breaking solutions as a function of an integration constant, α. For example, in the one constant approximation (all elastic constants are equal), the total free energy per unit length, $\mathscr{F}$, for a nematic liquid crystal with these boundary conditions and neglecting a constant surface term [8] that does not contribute to the dynamics, is

$$\frac{\mathscr{F}}{\pi K} = \frac{1}{\sin\alpha}\{2\mathscr{E}(\alpha) - \cos^2\alpha\mathscr{K}(\alpha)\}\,, \tag{1}$$

where $\mathscr{K}(\alpha)$ is the complete elliptic function of the first kind and $\mathscr{E}(\alpha)$, of the second kind [18]. We make use of this result (Eq. (1) shown in Fig. 2) later.

The lowest energy solutions are static solitons when $\alpha = \pi/2$ in which case $\hat{\mathbf{n}}$ radial at $r = R$ and either parallel or antiparallel to the cylinder axis, $\hat{\mathbf{z}}$, at $r = 0$, i.e., $\mathscr{G}(r) = \cot(\pi/4 + \phi/2)$ with $\mathscr{G}(r) = r/R$ for $0 \leqslant \phi \leqslant \pi/2$ and $\mathscr{G}(r) = R/r$ for $0 \geqslant \phi \geqslant -\pi/2$.

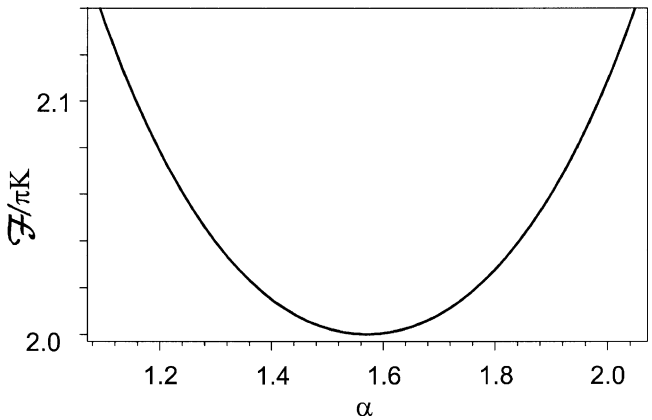

Fig. 2. Graph of Eq. (1), $\mathscr{F}/\pi K$ vs. α, shows that when the constant of integration $\alpha = \pi/2$, the energy of the system is at a minimum. But as the minimum is shallow, only a small perturbation is needed to drive a static soliton where $\hat{\mathbf{n}}$ is radial at $r = R$ and axial at $r = 0$ ($\alpha = \pi/2$), to a more energetic state where $\hat{\mathbf{n}}$ is radial at $r = R$ but axial in the region $r < r_o \neq 0$ ($\alpha \neq \pi/2$), where r_o is also determined only by α (Eq. (2

ϕ is the inclination of $\hat{\mathbf{n}}$ to the $r-\varphi$ plane (Fig. 1a) [19], Point defects are formed when these two lowest energy solutions (also known as "escaped" solutions in the liquid crystal literature) meet (Fig. 1b). When $H\bar{H}$ pairs annihilate, they leave behind a static soliton (Fig. 1d).

The hedgehog (H) consists of only splay deformation while its "antiparticle", the antihedgehog ($\bar{H}$), has both splay and bend (Fig. 1b). The elastic energy of an isolated $\bar{H}$ is about a third that of H with energy per unit length comparable to that of the static solitons on either side of it (Fig. 1b) (see footnote 2). This is a surprising result (published here for the first time) and another important difference between line defects and point defects: disclination lines with the same strength but opposite topological charge always have the same energy in the one constant approximation. We will attribute the unexpected more sluggish $\bar{H}$ dynamics compared to that of H during $H\bar{H}$ pair annihilation to the closeness of the $\bar{H}$ energy to that of the static soliton.

To stimulate H or $\bar{H}$ motion, it is necessary and sufficient that the energy on one side of the point defect be larger than on the other (Fig. 1c). Failing this, there is no force to drive the point defects to annihilate: they are asymptotically free [11](see footnote 2).

While static properties of point defects are relatively well known [10–12,20,21], interest in their dynamics is recent [9,22,23]. However, there is no previous work that has foreseen that hedgehog–antihedgehog annihilation dynamics is asymmetric. In addition, Refs. [22,23] accounted for point defect motion in their data by assuming that the boundary conditions were not radial as they are in this work. As a result, their point defects can never be asymptotically free whereas, as we will show here, ours can be.

3. The experiment

To facilitate optical analysis using a polarizing microscope interfaced through a video-camera to a computerized image analysis system, cylindrical glass capillaries are surrounded by an oil with the same index of refraction. The inner capillary wall, diameter, $d=2R$ with 60 μm $\leqslant d \leqslant$ 150 μm, was prepared so that $\hat{\mathbf{n}}$ is radial at $r=R$. The compound chosen was 8O CB (octyloxycyano-biphenyl) because the dramatic temperature dependence of its material constants are well known.[3] In 8O CB, $T_{NI}=79.6°$C and $T_{NA}=66.4°$C. The reduced temperature, ϑ, is $\vartheta \equiv (T-T_{NA})/(T_{NI}-T_{NA})$.

To initiate annihilation by induction of a slightly higher energy director configuration in the space between an $H\bar{H}$ pair (Fig. 1c), a sufficiently large external perturbation is required. The perturbation we employ is a temperature change. Depending on the magnitude, rate and direction i.e., increasing or decreasing temperature, an $H\bar{H}$ pair is prepared to annihilate. The data are then taken at constant temperature. The perturbation-induced higher energy state between $H\bar{H}$ pairs (Fig. 1c) relaxes much slower than any characteristic time for this system (see footnote 3).

[3] For measurements of K_3 and K_1, see for example, Ref. [24]. With the γ_1 measurements of Graf et al. we estimate for bend diffusion, $D_3=K_3/\gamma_1 \sim 1.7\times10^{-6}$ cm^2/s with characteristic time, $\tau_3 \sim 21$ s when $R=60$ μm and $\vartheta=0.4$. Reducing R by a factor of 2, decreases τ_3 by a factor of 4 for the same D_3.

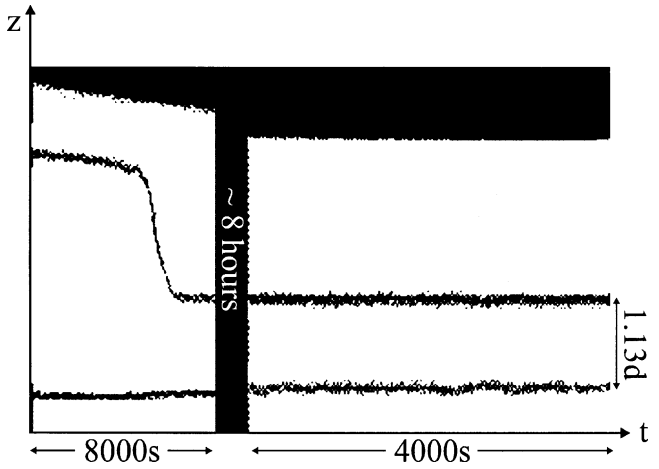

Fig. 3. $z_{\pm} - t$ plot showing asymptotic freedom for a static $H\bar{H}$ pair separated by more than a diameter, d (see footnote 2). The defect separation in the 8-h gap is identical to that shown for the last 4000 s. Here the capillary diameter is $d = 61.2$ μm which is very thin.

The position, $z_{+}(t)$ and $z_{-}(t)$, of the H and $\bar{H}$ defect cores, respectively, is simultaneously tracked as a function of time, t. This method reveals differences in $H\bar{H}$ dynamics and precisely establishes count-down to $t = 0$ and annihilation. As a result, throughout this paper, we define t as the time to annihilation so that larger t corresponds to larger $H\bar{H}$ separation and relatively weaker interactions than when t is smaller.

In these $z_{\pm} - t$ space–time plots, the point defect cores appear as lines in time separated by a region where $\hat{\mathbf{n}} \| \hat{\mathbf{z}}$ (Fig. 1c). In previous work [9,22,23], only the distance between H and $\bar{H}$ (i.e., $z_{+}(t) - z_{-}(t)$) is measured which gives no information about the asymmetry intrinsic to $H\bar{H}$ dynamics.

Fig. 3 shows a $z_{\pm} - t$ plot for an $H\bar{H}$ pair at $\vartheta \sim 0.81$ for a small initial perturbation such that $|z_{+}(t) - z_{-}(t))| \rightarrow 2.26R$ rapidly then stays there. As can be seen, the distance between H and $\bar{H}$ cores is constant for more than 12 h: a static pair of axially symmetric $H\bar{H}$ defects sufficiently far apart (Fig. 1b) has no attractive force [9,11,12]. This demonstration of asymptotic freedom is important because it shows that $\hat{\mathbf{n}}$ is indeed radial at $r = R$ (Fig. 1b) and that the $H\bar{H}$ pair is not connected by ever shortening line singularities as they are for $m\bar{m}$ objects [13].

Fig. 4a is a typical example of annihilation dynamics of an $H\bar{H}$ pair in a "thick" capillary relatively far from T_{NA} after a small perturbation from equilibrium. A number of features immediately catch the eye. The first is the strong asymmetry in $H\bar{H}$ dynamics up to annihilation: H moves approximately twice as fast as $\bar{H}$. Fig. 4a shows that a nearly perfect fit is obtained for the data by

$$z = z_{\pm}^{(0)} + z_{\pm}^{(1)} \exp[-t/\tau_{\pm}] + v_{\pm} t \tag{2}$$

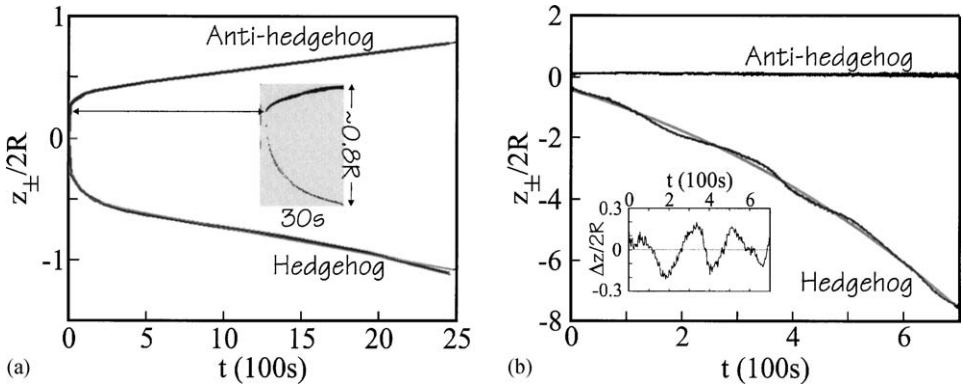

Fig. 4. Hedgehog and antihedgehog $z_{\pm} - t$ plots, $z_{\pm}/2R$, as a function of time, t. Annihilation is at $t = 0$, arrow in (a), which is not a fit parameter. When $H\bar{H}$ separation is $\lesssim 2R$, they move faster. The inset in (a) shows the hedgehog leaping towards the antihedgehog in the last ~0.5 s before annihilation at $\lesssim R/2$ separation. (a) "Thick" capillary—$d = 149$ μm, $\vartheta \sim 0.42$, weak perturbation ($\alpha \sim \pi/2$). The good fits to the data (thinner line) show that the annihilation dynamics of asymptotically free $H\bar{H}$ pairs is asymmetric and driven. Fits to the data are: $z_+/2R = -1 + 0.63\exp(-t/13) - 1.63 \times 10^{-3}t$ for the hedgehog and $z_-/2R = 0.47 - 0.33\exp(-t/25) + 0.43 \times 10^{-3}t$ for the antihedgehog. The $\bar{H}$ relaxation time is nearly twice as long as, and, its speed about a quarter, that of H. (b) "Thin" capillary—$d = 61.2$ μm, near $T_{NA}(\vartheta \sim 0.05)$, large initial perturbation ($\alpha \geqslant 2.5$). Strong layering fluctuations immobilize $\bar{H}$. The H data fits (thinner line) a single exponential: $z/2R = 3.3 - 11\exp(t - 700)/661$. The inset in (b) shows temporal modulations attributable to a "slip–stick" motion of the hedgehog core as it traverses smectic A fluctuations (see footnote 4). While the time scales in (a) are within expectations [24], those in (b) are much longer.

with the subscript $+$ referring to the hedgehog and $-$ to the antihedgehog. Here, $z_{\pm}$ is in units of $2R$, t in seconds, and $\tau_{\pm}$ is a characteristic director relaxation time which need not be the same for H and $\bar{H}$.

Fig. 4a shows that the $H\bar{H}$ fit: (1) is asymmetric; (2) covers nearly four decades in time: $0.3\text{ s} < t < \sim 2.5 \times 10^3$ s and (3) has both a linear regime when the $H\bar{H}$ pair is separated by more than a diameter and an exponential regime when $|z_+ - z_-| < 2R$. On the basis of more than 20 measurements at a variety of temperatures and capillary diameters, we conclude that the annihilation dynamics of $H\bar{H}$ pairs is driven and asymmetric.

In the "thinner" capillary close to T_{NA} (Fig. 4b), the antihedgehog is pinned even after a large initial perturbation, $\alpha \geqslant 140°$. In contrast, the hedgehog response to this same perturbation applied at t_∞ is a single exponential relaxation with a long-time constant dwarfing its behavior at $t \sim 0$. There is also a superposed temporal modulation shown inset in Fig. 4b after the exponential fit at t_∞ is subtracted from the data. While not strictly periodic, a mean time scale, $\tau_h \sim 250$ s, emerges. We attribute this temporal modulation to a "slip–stick" motion of the hedgehog's core as it traverses large amplitude smectic A fluctuations.[4] Oscillations are not observed near T_{NI}.

[4] Core model is a volume V_c of isotropic liquid. Energy to transform V_c is $\propto$ *Latent heat* $\times\, 4\pi r_c^3/3$. Minimizing the hedgehog energy against this energy gives $r_c \sim 67$ Å~twice the $8O$ CB smectic layer spacing.

4. The model

To model observations far from T_{NA} (e.g. Fig. 4a), we start by considering Eq. (1). Fig. 2 shows that the energy increase above that of a static soliton ($\alpha = \pi/2$) is small, e.g. less than 0.3% for $\alpha \sim 95°$ and $\sim 2\%$ for $\alpha \sim 108°$.

The sketch for $H\bar{H}$ dynamics in Fig. 1c is in the limit where $\alpha \sim \pi/2$. On the less energetic sides of the $H\bar{H}$ cores, $\hat{\mathbf{n}}$ is radial at $r = R$ and rotates smoothly to be axial at $r = 0$. In the perturbation-induced slightly more energetic region between them, $\hat{\mathbf{n}}$ is radial at $r = R$ and axial at $r_o > 0$ given by

$$r_o/R = \exp(-\sin\alpha \mathscr{K}(\alpha)), \quad 0 \leqslant \alpha \leqslant \frac{\pi}{2}\,. \tag{3}$$

When $\alpha = 0$, $r_o = R$ and, when $\alpha = \pi/2$, $\mathscr{K}(\pi/2) \to \infty$, so $r_o = 0$.

In the region $r \leqslant r_o$, $\hat{\mathbf{n}}$ is uniform and axial i.e., costs no energy. However, with this core structure, the $H\bar{H}$ point defect cores move $\|\hat{\mathbf{n}}$, i.e., through smectic A fluctuations that increase in amplitude as $T \to T_{NA}$ (see footnote 4) which would be qualitatively consistent with "slip–stick" modulations observed in Fig. 4b.

We interpret Fig. 4a, a typical example of annihilation dynamics of an $H\bar{H}$ pair, in the following way. We think of an (r, ϕ)-plane containing the defect core. When the energy on both sides of this plane is the same, there is no net force to move the defect (e.g. Fig. 1b). If on one side of the plane, r_o is nonzero while on the other, $r_o = 0$, there is a net force pushing the defect to replace the $r_o \neq 0$ region by the less energetic $r_o = 0$ region, and the defect moves (Figs. 1c and 2).

In Fig. 4a, then, this model would say that the hedgehog speed is nearly four times faster than that of the antihedgehog because it is nearly three times more energetic and has a larger r_o (Fig. 1c) than the antihedgehog.

While τ_+ could be half τ_- close to the smectic A transition, it is not expected to be so different at the temperature of Fig. 4a where all the visco-elastic coefficients are comparable. Rather we suggest that the relaxation of $\bar{H}$ to $\pi/2$ could be preempted by the hedgehog arriving at the point of annihilation before antihedgehog relaxation has completely taken place (see inset in Fig. 4a). Loosely speaking, H and $\bar{H}$ travel towards each other at different speeds such that annihilation takes place closer to the antihedgehog so that it may not have a chance to relax to equilibrium before the hedgehog runs into it.

The only length scale in this model for $H\bar{H}$ dynamics is thus r_o which is determined only by α. If $r_o = 0$, the point defects do not interact (are asymptotically free—e.g. Figs. 1b and 3). If $r_o \neq 0$ in the region between the point defects, they move along the axial energy gradient to reduce the total energy of the system. They move at different speeds because the driving force for the hedgehog is larger than it is for the antihedgehog.

The simplest assumption is to take $r_o \propto z_\pm$ with r_o larger in the vicinity of the hedgehog and smaller in the vicinity of the antihedgehog. This gives rise to a constant induced drift speed for the defects but one which is larger for the hedgehog and smaller for the antihedgehog.

One then has two regimes for the dynamics: a regime at large times with a drift determined by the external perturbation and a second regime as $t \to 0$ where the

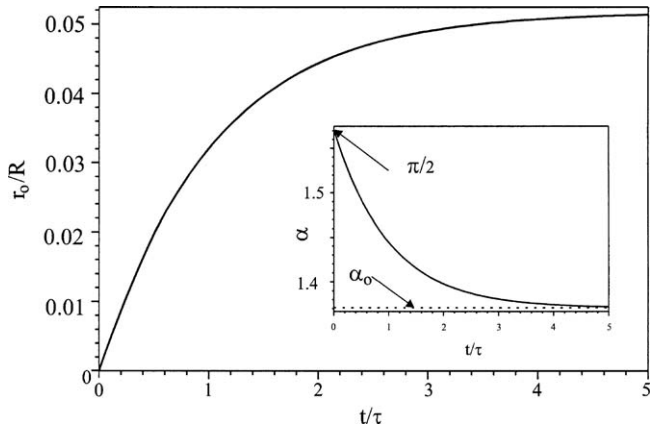

Fig. 5. In this plot, annihilation takes place at $t = 0$ which is well defined in the experiment. Thus, small time, t, corresponds to when H and $\bar{H}$ are close to each other and their interaction is largest while large t corresponds to when they are separated by more than $2R$ where their interaction is weakest. The larger graph shows r_o/R versus t/τ, with the graph of Eq. (4) shown in the inset. In this plot, $\alpha_o = 1.3708 = 78.5°$. As $t \to 0$ and annihilation, $\alpha \to \pi/2$. $\pi/2$ is equilibrium for this system. At long times, $\alpha \sim \alpha_o \neq \pi/2$ is determined by the initial perturbation and is nearly constant.

relaxation of $r_o \to 0$ dominates (Fig. 4a). The cross-over length between these two regimes is when $|z_+ - z_-| \sim 2R$. If $r_o = 0$ and the $H\bar{H}$ pair separation is larger than $2R$, that is $|z_+ - z_-|_{t\to\infty} > 2R$, the force driving their annihilation has disappeared. As a result, the $H\bar{H}$ pair no longer interact i.e., they are asymptotically free (Fig. 3).

The experimental results in Fig. 4 are presented as a count-down to annihilation such that $t = 0$ at annihilation. Thus, shorter times correspond to closer distances between H and $\bar{H}$ and therefore larger interactions while longer times correspond to larger separations and weaker interactions. The perturbation that pushes α out of equilibrium takes place at a long time ($t \to \infty$) before annihilation where the H and $\bar{H}$ are separated by much more than $2R$. The separation $2R$ is crucial: those $H\bar{H}$ pairs that are closer than $2R$ when $\alpha \neq \pi/2$ have to annihilate exponentially fast (Fig. 4a). Should α reach $\pi/2$ when the $H\bar{H}$ pair is separated by more than $2R$, they are asymptotically free (Fig. 3).

α relaxes to $\pi/2$ from $\alpha_o \neq \pi/2$ set at some long time, $t \gg \tau$. That is, for larger (but still small) perturbations, we put

$$\alpha = \alpha_o + (\pi/2 - \alpha_o)\exp(-t/\tau)\ . \tag{4}$$

Eq. (4) is shown as an inset in Fig. 5. At time $t \to \infty$ i.e., far from annihilation where the $H\bar{H}$ separation is much larger than $2R$, $\alpha = \alpha_o$ and at time $t = 0$, i.e., at annihilation, $\alpha = \pi/2$. For t/τ greater than about 5, α is nearly constant and equal to α_o. It is only when H and $\bar{H}$ are sufficiently close to each other (within $2R$) where their interactions become increasingly stronger that the exponential behavior for $\alpha \to \pi/2$ kicks in, in agreement with the observations (e.g. Fig. 4a).

Including a drift velocity, v, in $z_{\pm}$ we arrive at Eq. (2). The solid lines in Fig. 4 show that this simple picture (Eq. (2)) provides an excellent fit to our experimental data far from T_{NA} (Fig. 4a).

In striking contrast, there is no drift term in Fig. 4b where the data is taken in a "thin" capillary very close to T_{NA} where $H\bar{H}$ dynamics is controlled by large amplitude layering fluctuations: the antihedgehog is stationary while the hedgehog shows only an exponential decay to annihilation. The one constant approximation clearly breaks down.

To observe $H\bar{H}$ pair annihilation in thin capillaries, a significantly large perturbation is required. For hedgehogs, the temporal extent of the drift term decreases as $T \to T_{NA}$ and Eq. (2) no longer applies below $\vartheta \sim 0.6$. Antihedgehogs can be fit to Eq. (2) for all ϑ but only in a decreasingly smaller time interval to annihilation as $T \to T_{NA}$. Thus, a full 2D calculation seems necessary to account for $H\bar{H}$ dynamics in thin capillaries e.g. Fig. 4b. These calculations would not only have to take into account the fact that the elastic constant for bend, K_3, is much larger than that for splay, K_1, but also the fact that some of the viscous coefficients not only diverge but also change sign as $T \to T_{NA}$ [17].

5. Conclusions

In conclusion, $H\bar{H}$ dynamics depends sensitively on the magnitude of the perturbation triggering pair annihilation. For a sufficiently small perturbation, the system shows asymptotic freedom (Fig. 3). For sufficiently large perturbations, hedgehog–antihedgehog pair annihilation dynamics has a regime dominated by elastic relaxation where $H\bar{H}$ separation is less than $2R$ and a perturbation induced drift regime when $H\bar{H}$ separation is much larger than $2R$ (Fig. 4a). $H\bar{H}$ dynamics is highly asymmetric because of the larger "effective mass" of the antihedgehog. This asymmetry persists up to annihilation and is most dramatic near T_{NA} where the antihedgehog is pinned (Fig. 4b) and is more energetic than either the hedgehog or the static soliton. Hedgehog–antihedgehog pairs are especially suited to test understanding of point defect core structures as well as defect dynamics in effectively one spatial dimension.

Acknowledgements

We thank Elliott Lieb for stimulating discussions.

References

[1] P.E. Cladis, Y. Couder, H.R. Brand, Phys. Rev. Lett. 55 (1985) 2945.
[2] P.E. Cladis, P.L. Finn, H.R. Brand, Phys. Rev. Lett. 75 (1995) 1518.
[3] P. Poulin, V. Cabuil, D.A. Weitz, Phys. Rev. Lett. 79 (1997) 4862.
[4] C. Fradin, P.L. Finn, H.R. Brand, P.E. Cladis, Phys. Rev. Lett. 81 (1998) 2902.
[5] I. Chang, N. Turok, B. Yurke, Phys. Rev. Lett. 66 (1991) 2472.

[6] V.M. Ruutu, V.B. Eltsov, A.J. Gill, T.W. Kibble, M. Krusius, Y.G. Makhlin, B. Placais, G.E. Volovik, W. Xu, Nature 382 (1996) 334;
C. Bäuerle, Y.M. Bunkov, S.N. Fisher, H. Godfrin, G.R. Pickett, Nature 382 (1996) 332.
[7] W.H. Zurek, Nature 317 (1985) 505.
[8] P.E. Cladis, M. Kléman, J. Phys. (Paris) 33 (1972) 591.
[9] J.L. Ericksen, in: M.M. Carroll, M.A. Hayes (Eds.), Nonlinear Effects in Fluids and Solids, Plenum, New York, 1996, p. 137ff.
[10] C. Williams, P. Pieranski, P.E. Cladis, Phys. Rev. Lett. 29 (1972) 90.
[11] W.F. Brinkman, P.E. Cladis, Phys. Today 35 (5) (1982) 48.
[12] E.C. Gartland Jr., A.M. Sonnet, E.G. Virga, Continuum Mech. Thermodyn. 14 (2002) 307.
[13] A. Pargellis, N. Turok, B. Yurke, Phys. Rev. Lett. 67 (1991) 1570.
[14] P.E. Cladis, W. van Saarloos, P.L. Finn, A.R. Kortan, Phys. Rev. Lett. 58 (1987) 222.
[15] G. Toth, C. Denniston, J.M. Yeomans, Phys. Rev. Lett. 88 (2002) 105 504.
[16] D. Svensek, S. Zumer, Phys. Rev. E 66 (2002) 021712.
[17] P.E. Cladis, Fluctuations and liquid crystal phase transition, in: D. Demus, J. Goodby, G.W. Gray, H.-W. Spiess, V. Vill (Eds.), Physical Properties of Liquid Crystals, Wiley-VCH, Weinheim, 1999, p. 277.
[18] L.M. Milne-Thomson, in: M. Abramowitz, I. Stegun (Eds.), Handbook of Mathematical Functions, Dover Publications, Inc., New York, 1970, p. 587.
[19] P.E. Cladis, W. van Saarloos, Some nonlinear problems in anisotropic systems, in: L. Lam, J. Prost (Eds.), Solitons in Liquid Crystals, Springer, New York, 1991, pp. 110–150.
[20] Y. Bouligand, P.E. Cladis, L. Liébert, L. Strzelecki, Mol. Cryst. Liq. Cryst. 25 (1974) 233.
[21] A. Saupe, Mol. Cryst. Liq. Cryst. 21 (1973) 211.
[22] G.G. Peroli, G. Hillig, A. Saupe, E.G. Virga, Phys. Rev. E 58 (1998) 3259.
[23] G.G. Peroli, E.G. Virga, Phys. Rev. E 59 (1999) 3027.
[24] M.J. Bradshaw, E.P. Raynes, J.D. Bunning, T.E. Faber, J. Phys. (Paris) 46 (1985) 1513;
H.-H. Graf, H. Kneppe, F. Schneider, Mol. Phys. 77 (1992) 521.